Electrical Sensitivity Optimization for 3D Impedance-Based Cancer Culture Systems: Experimental Property Extraction and Simulation Modeling

Gerard Lorio
Advisors: Dr. Todd Monroe and Dr. Jorge Belgodere

Honors BE 4390, 2026 Fall Semester
December 8, 2025

This work represents an individual, non-overlapping investigation derived from the senior design project, focused specifically on the electrical sensitivity optimization via electrode–scaffold spacing.

Abstract

Impedance spectroscopy enables real-time, label-free assessment of cell viability, but its effectiveness in 3D scaffolds is reduced due to limited electric-field penetration compared to conventional 2D systems. In 3D cultures, cells are embedded within a bulk hydrogel rather than directly contacting electrodes, causing current to preferentially travel through surrounding media and decreasing sensitivity to biological changes. The objective of this work was to establish quantitative geometric design guidelines that preserve interrogation sensitivity in realistic 3D microphysiological environments. Electrical properties of PEDOT:PSS hydrogels and fish-gelatin methacrylate (fGelMA) scaffolds were experimentally measured using a custom parallel-plate device and an Agilent E4980A LCR meter. Conductivity and permittivity values were incorporated into COMSOL Multiphysics® simulations (Electric Currents interface) to model frequency-dependent current transport through the scaffold and media. Electrode-to-scaffold separation distances from 0 to 3.5 mm were evaluated to determine their impact on detecting impedance differences between live-like and dead-like scaffold conditions. Simulation outputs were analyzed in Python to extract impedance magnitude, phase, and Nyquist behavior, and sensitivity was quantified as the peak percent change in impedance magnitude ($\Delta|Z|$). Results demonstrated that electrode proximity is the dominant factor governing measurement performance. Direct electrode–scaffold contact (0 mm gap) yielded 32.4% $\Delta|Z|$, enabling clear discrimination between scaffold states. As media separation increased, electric-field penetration rapidly declined, and sensitivity fell below 10% for gaps ≥3.0 mm. These findings validate the design hypothesis and establish a key engineering guideline for 3D impedance systems: electrode separation must be ≤1 mm to maintain biologically meaningful interrogation. This modeling framework provides actionable guidance for future 3D cancer culture devices and reduces prototyping time by predicting performance prior to fabrication.

Table of Contents

1. Introduction

1.1. Background

Impedance spectroscopy is a label-free method capable of continuously monitoring cell behavior, and it has been extensively validated in 2D monolayer cultures where cell–electrode contact is direct and the corresponding electrical response is well understood[1]. However, 2D systems lack critical physiological features of the tumor microenvironment, including extracellular matrix interactions, structural confinement, and gradients in nutrients and waste, leading to inaccurate prediction of in vivo drug response[2]. As a result, 3D culture platforms—such as spheroids, hydrogels, and microphysiological systems—are increasingly used for disease modeling because they better recapitulate native tissue architecture and cell–ECM interactions[3]. Extending impedance-based sensing into 3D systems offers the opportunity to monitor viability and treatment response in real time and without sample destruction[4].

1.2. Problem Statement

Unlike 2D cultures, cells in 3D reside within a bulk matrix rather than directly on the electrode surface. The electric field must therefore propagate through a heterogeneous environment consisting of media, polymer, and cellular regions, each with distinct dielectric properties[5]. When 3D scaffolds are extremely small. or when spheroids span directly between two electrodes, impedance changes remain highly sensitive to viability[6]. However, these geometries artificially restrict biological growth and limit cell numbers. Increasing electrode spacing to support physiologically relevant scaffold sizes causes the electric field to decay and divert through lower-resistance fluid regions[5], making the signal dominated by bulk media instead of cell-dependent pathways. This loss of field density reduces sensitivity to viability-driven changes and results in unpredictable performance.

1.3. Measurable Objectives

This work aims to establish quantitative design guidelines that maximize the sensitivity of impedance-based interrogation in realistic 3D cell culture environments. First, the electrical properties of project-relevant materials will be characterized by extracting conductivity (σ) and relative permittivity (ε_r) from impedance measurements of PEDOT:PSS hydrogels at multiple percent weight concentrations, as well as fGelMA scaffolds under soaked and unsoaked conditions. These properties will be reported at a representative frequency (2 MHz) with a target variability of $\leq 10\%$ across at least three independent replicates. Next, the experimentally derived σ and ε_r values will be directly incorporated into COMSOL Multiphysics® models to simulate electric-field propagation and composite impedance response within the 3D culture environment. Interrogation performance will be systematically evaluated across a practical design space by varying electrode spacing from 0–3.5 mm, where 0 mm represents direct electrode contact and 3.5 mm reflects the maximum separation allowed by fabrication constraints. because 0 marks the least possible gap while 3.5 marks the greatest possible gap that is possible to fabrication. Sensitivity will be quantified using impedance magnitude ($\Delta|Z|$) and phase shift ($\Delta\emptyset$) between “live-like” and “dead-like” conditions, with a performance target of at least a 20% increase in $\Delta|Z|$ for the optimized geometry compared to the largest separation distance. Finally, the results will be synthesized to identify an optimal interrogation configuration that balances manufacturability and sensing performance.

The success criterion is to establish a geometric design window that yields ≥ 25% impedance contrast between viability conditions.

1.4. Constraints

To maintain compatibility with microphysiological devices and manufacturable workflows, the system is limited to materials that can be fabricated using standard lab equipment. For this reason, Poly(E)thylene Dioxythiophene : Poly(S)tyrene Sulfonate (PEDOT:PSS) was selected as the conductive phase due to its flexibility, conductivity tunability, and biocompatibility for long-term culture[8]. Poly(E)thylene Glycol DiAcrylate (PEGDA) provides a soft, tissue-like hydrogel structure with mechanical stability[9]. PEDOT:PSS-PEGDA composite electrodes have demonstrated the ability to support cell viability while enabling efficient electrical communication with surrounding tissues[10], ensuring that any optimized interrogation strategy can be implemented in a biologically relevant 3D environment.

2. Methods

2.1. Relative Electrical Interrogator

To inform the electrical modeling in COMSOL, the conductivity (σ) and relative permittivity (ε_r) of materials relevant to this system were experimentally quantified. The materials evaluated included multiple concentrations of PEDOT:PSS (% w/v) and fish-gelatin methacrylate (fGelMA) scaffolds in both media-soaked and unsoaked conditions. A parallel-plate interrogation device was fabricated using polylactic acid (PLA) via fused deposition modeling (FDM) on an A1 Mini 3D printer (Bambu Lab, Shenzhen, CH). The device consisted of two identical magnetic halves with an embedded glass slide to provide a rigid backplane and alignment. Each half contained a rectangular interrogation cavity (≈ 4 mm gap × 6 mm width × 2 mm height), with the inner walls used for copper tape to reference to form the working and reference electrode plates. A thin Kapton® film was applied over the copper to prevent direct shorting between plates during compression (ULINE, Wisconsin, USA). Material specimens were fabricated to a height of ~4.5 mm to extend 0.5 mm above the cavity height, such that light magnetic compression ensured full electrode–material contact and eliminated air gaps. The copper tape paths were connected to shielded leads which were connected to a female connector compatible with the E4980A Precision Inductance-Capacitance-Resistance (LCR) Meter (Agilent Technologies, Santa Clara, US). The LCR meter supplied a 50 mV AC excitation across a 200 MHz with logarithmic step of 200 and measured resistance (R) and reactance (X). These values were used to compute conductivity and relative permittivity using standard parallel-plate relationships:

$$\varepsilon_t = \frac{Cd}{\varepsilon_0 A} \qquad \text{(Eqn. 1)}$$

$$\sigma = \frac{d}{RA} \qquad \text{(Eqn. 2)}$$

Given the constant parameters – plate separation (d, 4 mm), vacuum permittivity (ε_0, 8.854x10^{-12} F/m), and electrode area (A, 18 mm^2) – the equations simplified to:

$$\varepsilon_r = 1.88x10^{10}C, \text{ where } C = \frac{1}{2\pi f|X|} \qquad \text{(Eqn. 3)}$$

$$\sigma = \frac{1.67x10^2}{R} \qquad \text{(Eqn. 4)}$$

Thus, reactance ($|X|$) and resistance ($|R|$) measured by the LCR meter were directly converted to relative permittivity and conductivity using Equations 3 and 4.

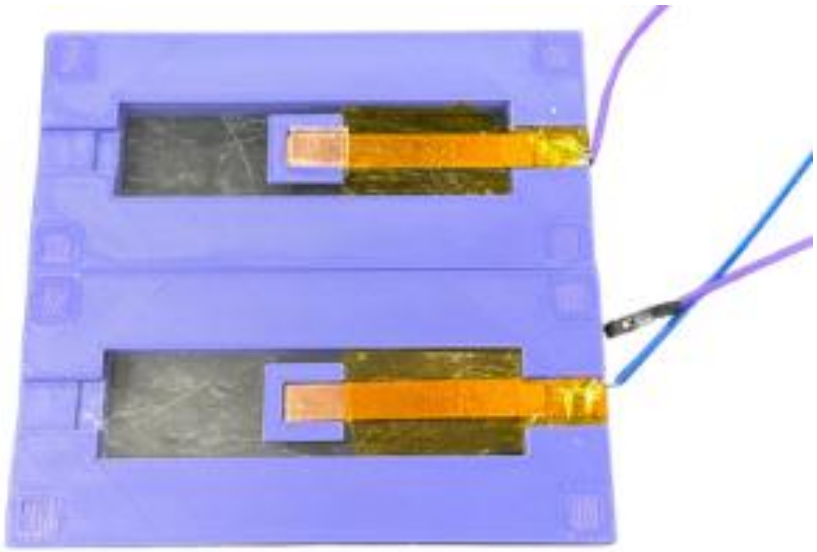

Figure 1. Fabricated interrogation device featuring embedded magnets, a glass substrate, copper electrodes, Kapton insulation, and wired connection to the LCR meter.

2.2. COMSOL Setup

Solid model components of the impedance interrogation system—including the PEDOT:PSS–PEGDA electrodes, copper conduction layer, media channel, and fGelMA scaffold—were designed in Fusion CAD software (Autodesk, San Francisco, CA, USA) and imported into COMSOL Multiphysics® for simulation. The Electric Currents physics interface (AC/DC Module) was used to solve frequency-dependent current transport and electric field distribution throughout the 3D culture environment. Material domains were assigned experimentally informed conductivity (σ) and relative permittivity (ε_{r}) values using parametric switching to represent viable-like and dead-like scaffold conditions. The exact values entered into COMSOL were described in Table 1.

Table 1. Electrical properties used in COMSOL simulations.

Material	σ (S/m)	ε_r
Complete Media	1.5×10^{-2}	80
Soaked fGelMA (Alive-like)	5.5×10^{-7}	50
Soaked fGelMA (Dead-like)	3.5×10^{-7}	50
PEDOT:PSS—PEGDA	10	40
Copper Tape (electrode layer)	5.96×10^{7}	1

A parametric sweep was implemented to toggle scaffold electrical properties between live-like and dead-like states using Boolean control variables ($alive = 1, dead = 0$). Boundary conditions were defined such that one copper tape electrode surface that runs underneath the PEDOT:PSS—PEGDA was assigned a Terminal boundary with a 50 mV AC excitation, while the opposite copper pathing was set to Ground (0 V). Direct electrical contact was enforced between the scaffold and electrode surfaces to allow realistic charge transfer, and all remaining exterior boundaries were treated as electrically insulating ($n \cdot J = 0$) to prevent current leakage from the model. A Frequency-Domain study was performed with a swept excitation from 200 Hz to 2 MHz to match the experimental interrogation conditions. From this study, COMSOL outputs included impedance magnitude ($|Z| = abs(1/ec.Y11)$), impedance phase ($arg(1/ec.Y11)$), and terminal current ($ec.I0$). Additionally, spatial mapping of electric-field magnitude ($|E|$) was used to quantify field penetration depth within the scaffold volume. A geometric sensitivity sweep was also performed in which the electrode-to-electrode gap was varied from 0 mm to 3.5 mm in 0.5 mm increments to assess the effect of spacing on interrogation performance.

2.3. Data Analysis

To evaluate interrogation sensitivity across the simulated geometries, impedance spectra were exported from COMSOL and analyzed in Python. Three standard plots were generated for each electrode gap configuration: Bode magnitude ($|Z|$ vs. frequency), Bode phase ($\emptyset$ vs. frequency), and Nyquist ($-Imag(Z)$ vs. $Real(Z)$). A reliability window was defined based on the phase response, where scaffold-dependent differences were consistently detectable ($-0.20 \geq \emptyset \geq -0.70$ radians). Within this frequency region, the maximum absolute difference between alive-like and dead-like conditions was identified for each geometry. Sensitivity was quantified as the percent difference in impedance magnitude, calculated at the frequency where $\Delta|Z|$ peaked. This peak percent difference value was then compared across gap distances (0–3.5 mm) to determine how the amount of DMEM separation influences the scaffold-specific electrical signal.

3. Results and Discussion

The 2.5% PEDOT:PSS–PEGDA formulation was selected as the optimal sidewall-electrode material because it offered comparable permittivity to the 5% formulation while maintaining much better printability and mechanical integrity. Although the 5% formulation exhibited ~40% higher conductivity, it was significantly more brittle and difficult to fabricate.

As shown in Fig. 3, increasing the media gap between electrodes caused a substantial reduction in electric-field penetration through the fGelMA scaffold. When the electrodes were in direct contact with the scaffold (0 mm gap), the electric field remained concentrated within the hydrogel volume, ensuring that the interrogating current pathway strongly depended on the scaffold's electrical properties. However, as the media gap increased, the electric field increasingly shunts through the highly conductive media, bypassing the scaffold. This loss of field density within the scaffold core directly reduced the system's ability to detect viability-dependent differences.

This trend was quantitatively reflected in the maximum percent difference in impedance magnitude ($\Delta|Z|$) between alive-like and dead-like conditions. With a 0 mm gap, a sensitivity of 32.4% was achieved, demonstrating strong discrimination between scaffold states. Sensitivity then decreased monotonically with increasing gap: 24.1% (0.5 mm), 18.7% (1.0 mm), 14.9% (1.5 mm), 12.2% (2.0 mm), 10.1% (2.5 mm), and finally 8.6% for gaps ≥ 3.0 mm. At these larger separations, the alive and dead scaffolds became nearly electrically indistinguishable, indicating that interrogation no longer reflected cell-dependent conductivity. Together, these results confirmed that direct or near-direct contact between the electrodes and the scaffold was the most effective configuration, and that even millimeter-scale fluid separation severely compromised sensitivity in 3D impedance measurements.

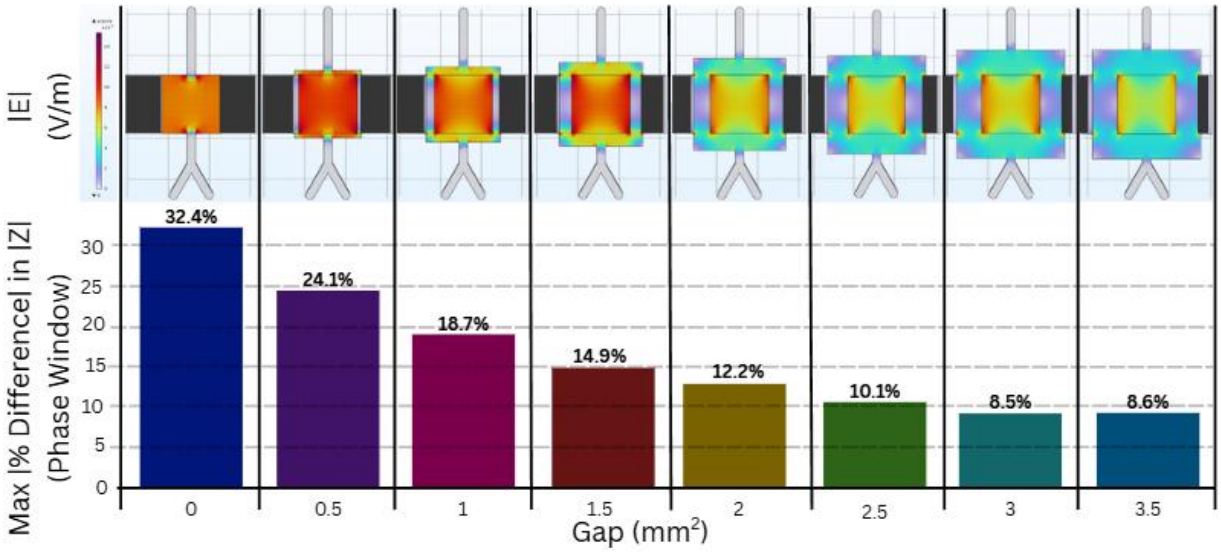

Figure 2. Electrode-scaffold gap length dependent (top) electric field and (bottom) impedance sensitivity using impedance difference between live and dead scaffolds.

4. Conclusion

This work successfully defined quantitative design rules for maximizing sensitivity in 3D impedance-based culture systems. Experimental material interrogation combined with multiphysics modeling demonstrated that electrode–scaffold contact was essential for resolving viability-dependent changes in impedance. When the scaffold directly contacted both electrodes, sensitivity peaked at 32.4% $\Delta|Z|$, whereas even a 1–3 mm media separation reduced contrast to ≤10%, effectively masking biological differences. These results confirmed the initial hypothesis and provided clear, actionable criteria for microphysiological system design: maintain ≤1 mm separation to ensure reliable interrogation. The validated modeling framework reduced trial-and-error in future device fabrication and can now be extended to more complex electrode layouts and volumetric cell-laden scaffolds. This will enable interrogation of viability gradients and signal density throughout 3D tumor constructs, advancing the development of high-fidelity cancer culture systems.

5. References

1. Duval, K., Grover, H., Han, L. H., Mou, Y., Pegoraro, A. F., Fredberg, J., & Chen, Z. (2017). Modeling Physiological Events in 2D vs. 3D Cell Culture. *Physiology (Bethesda, Md.)*, *32*(4), 266–277. https://doi.org/10.1152/physiol.00036.2016
2. Baptista, L. S., Porrini, C., Kronemberger, G. S., Kelly, D. J., & Perrault, C. M. (2022). 3D organ-on-a-chip: The convergence of microphysiological systems and organoids. *Frontiers in cell and developmental biology*, *10*, 1043117. https://doi.org/10.3389/fcell.2022.1043117
3. Wegener, J., Keese, C. R., & Giaever, I. (2000). Electric cell-substrate impedance sensing (ECIS) as a noninvasive means to monitor the kinetics of cell spreading to artificial surfaces. *Experimental cell research*, *259*(1), 158–166. https://doi.org/10.1006/excr.2000.4919
4. Hassan, Q., Ahmadi, S., & Kerman, K. (2020). Recent Advances in Monitoring Cell Behavior Using Cell-Based Impedance Spectroscopy. *Micromachines*, *11*(6), 590. https://doi.org/10.3390/mi11060590
5. Lei, K. F., Wu, M. H., Hsu, C. W., & Chen, Y. D. (2014). Real-time and non-invasive impedimetric monitoring of cell proliferation and chemosensitivity in a perfusion 3D cell culture microfluidic chip. *Biosensors & bioelectronics*, *51*, 16–21. https://doi.org/10.1016/j.bios.2013.07.031
6. Pan, Y., Jiang, D., Gu, C., Qiu, Y., Wan, H., & Wang, P. (2020). 3D microgroove electrical impedance sensing to examine 3D cell cultures for antineoplastic drug assessment. Microsystems & Nanoengineering, 6, Article 23. https://doi.org/10.1038/s41378-020-0130-x
7. COMSOL AB. (2024). *COMSOL Multiphysics*® (Version 6.2) [Computer software]. https://www.comsol.com
8. Lopez-Larrea, N., Criado-Gonzalez, M., Dominguez-Alfaro, A., Alegret, N., Agua, I. D., Marchiori, B., & Mecerreyes, D. (2022). Digital Light 3D Printing of PEDOT-Based Photopolymerizable Inks for Biosensing. *ACS applied polymer materials*, *4*(9), 6749–6759. https://doi.org/10.1021/acsapm.2c01170
9. Li, J., Mo, D., Hu, J. *et al.* PEDOT:PSS-based bioelectronics for brain monitoring and modulation. *Microsyst Nanoeng* **11**, 87 (2025). https://doi.org/10.1038/s41378-025-00948-w
10. Spencer, A. R., Primbetova, A., Koppes, A. N., Koppes, R. A., Fenniri, H., & Annabi, N. (2018). Electroconductive Gelatin Methacryloyl-PEDOT:PSS Composite Hydrogels: Design, Synthesis, and Properties. *ACS biomaterials science & engineering*, *4*(5), 1558–1567. https://doi.org/10.1021/acsbiomaterials.8b00135